

Fig. S1. *Magoh* mRNA is highly expressed within human and mouse interneuron progenitors. (A) *Magoh* expression from single cell sequencing of mouse E14.5 and P0 cortices (from (Loo et al., 2019)). Boxed region indicates relative expression within ganglionic eminences. (B) *Magoh* expression from single cell sequencing of human cortices. Circle indicates expression in MGE from (Nowakowski et al., 2017).

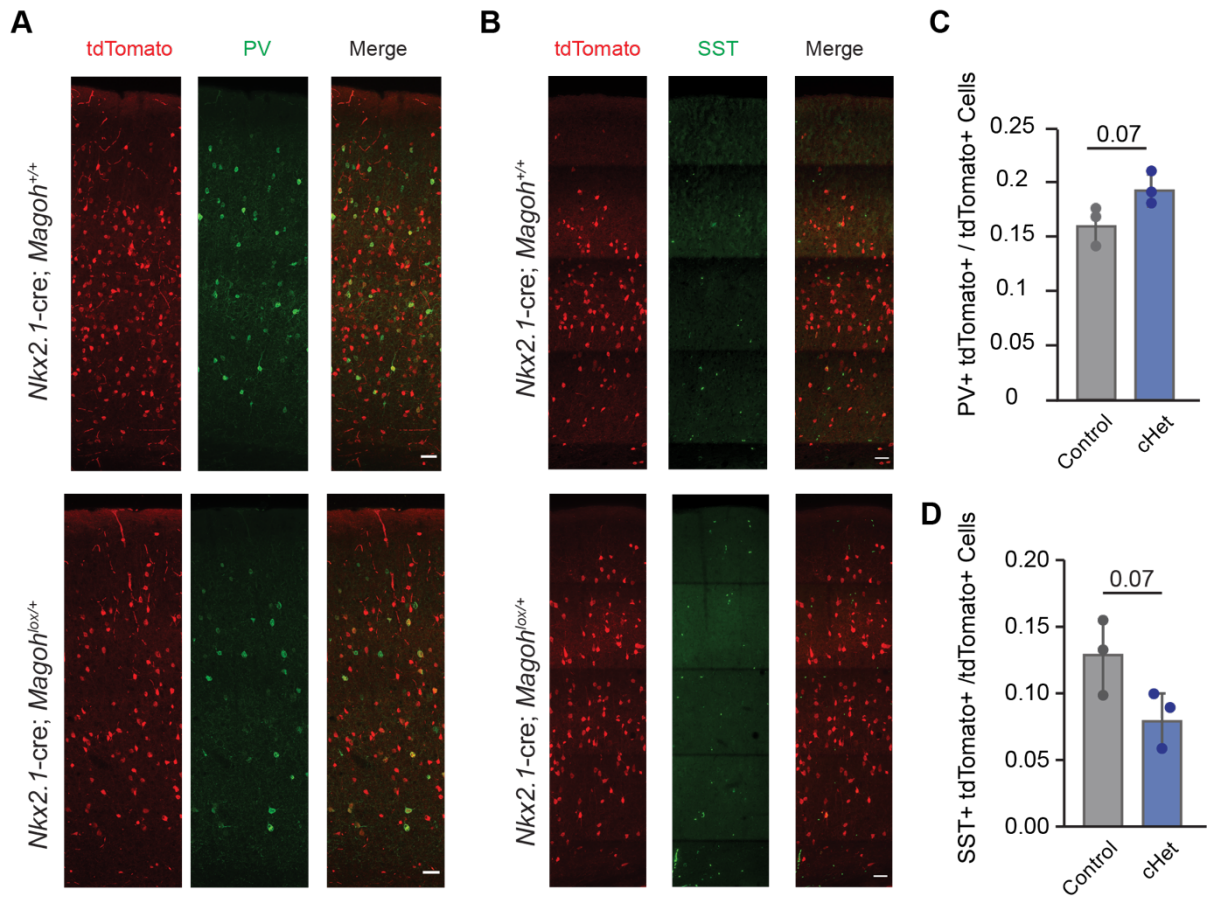


Fig. S2. Adult SST and PV interneuron subtype ratio show altered trends in *Magoh* conditional haploinsufficient adults. (A, B) Coronal sections of *Nkx2.1-cre* (top) and *Nkx2.1-cre; Magoh^{lox/+}* (bottom) P60 cortex co-stained for tdTomato (red) and parvalbumin (green) (A) or somatostatin (green) (B). (C,D) Fraction of *Nkx2.1-cre* derived PV (C) or SST (D) cells. Individual dots represent biological replicates. Two-tailed unpaired student t-test; $p=0.0736$ (C) and $p = 0.0706$ (D) Scale bars: A-B, 25 μ m.

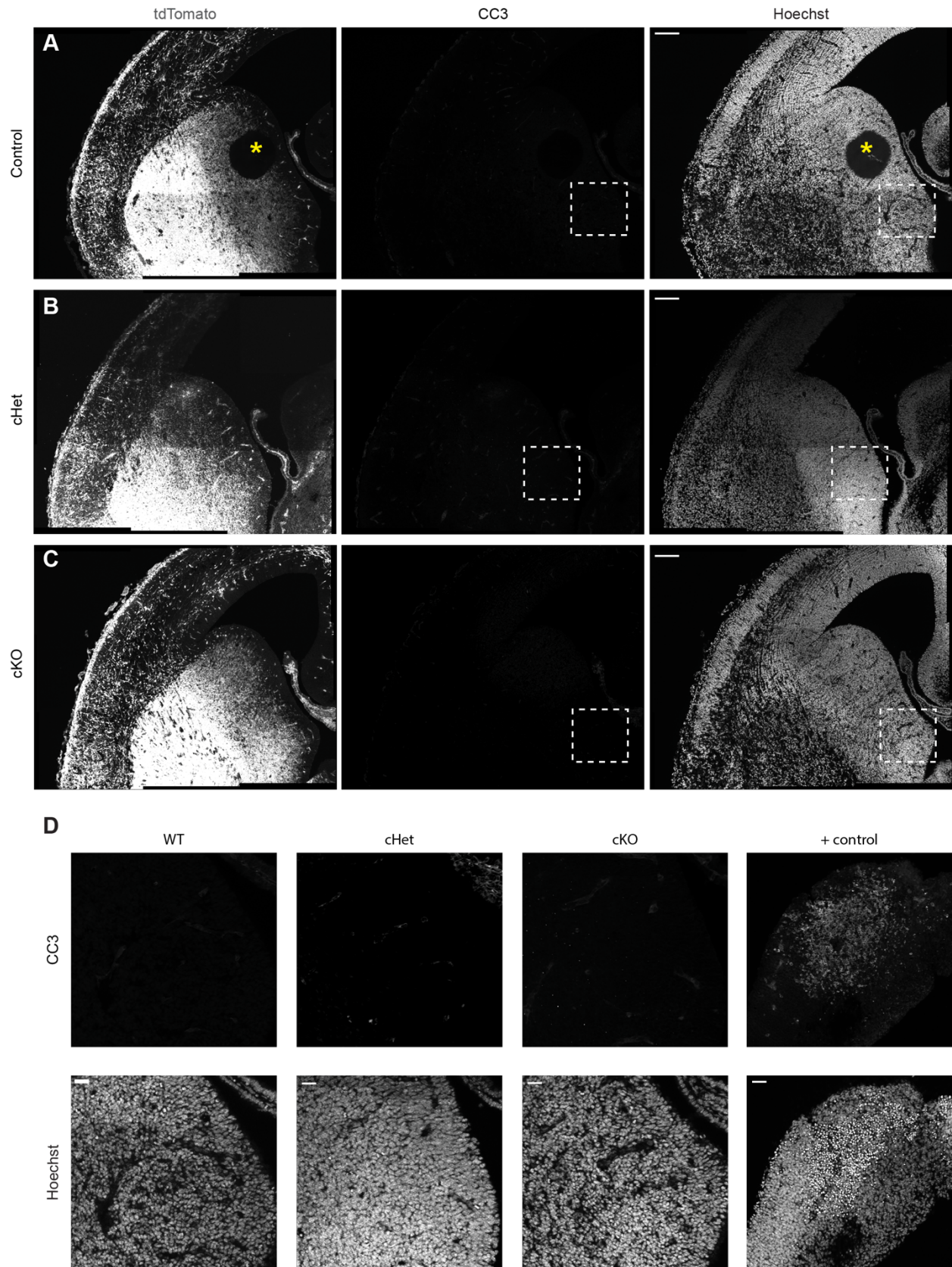


Fig. S3. *Dlx5/6*-Cre mediated *Magoh* depletion does not cause apoptosis or altered migratory patterns. (A-C) Representative coronal sections of E14.5 *Dlx5/6-cre;Rosa^{loxSTOPlxtdTomato}* (A) *Dlx5/6-cre; Magoh^{lox/lox};Rosa^{loxSTOPlxtdTomato}* (B), and *Dlx5/6-cre; Magoh^{lox/+};Rosa^{loxSTOPlxtdTomato}* (C) brains depicting tdTomato positive interneurons (grey/left) throughout the ventral telencephalon and migrating into the cortex. Immunostaining for cleaved caspase 3 (CC3)(grey/middle), an apoptosis marker, and Hoechst (white/right). (D) High magnification images of WT, cHet, and cKO medial ganglionic eminence (MGE) represented by boxed regions in (A-C) along with a positive control for CC3 staining (MGE of *Nkx2.1-cre; Magoh^{lox/lox}*). Note that amongst all genotypes, no apoptosis was evident and the pattern of migrating interneurons was similar. Scale bars: A-C, 145µm; D, 25µm.

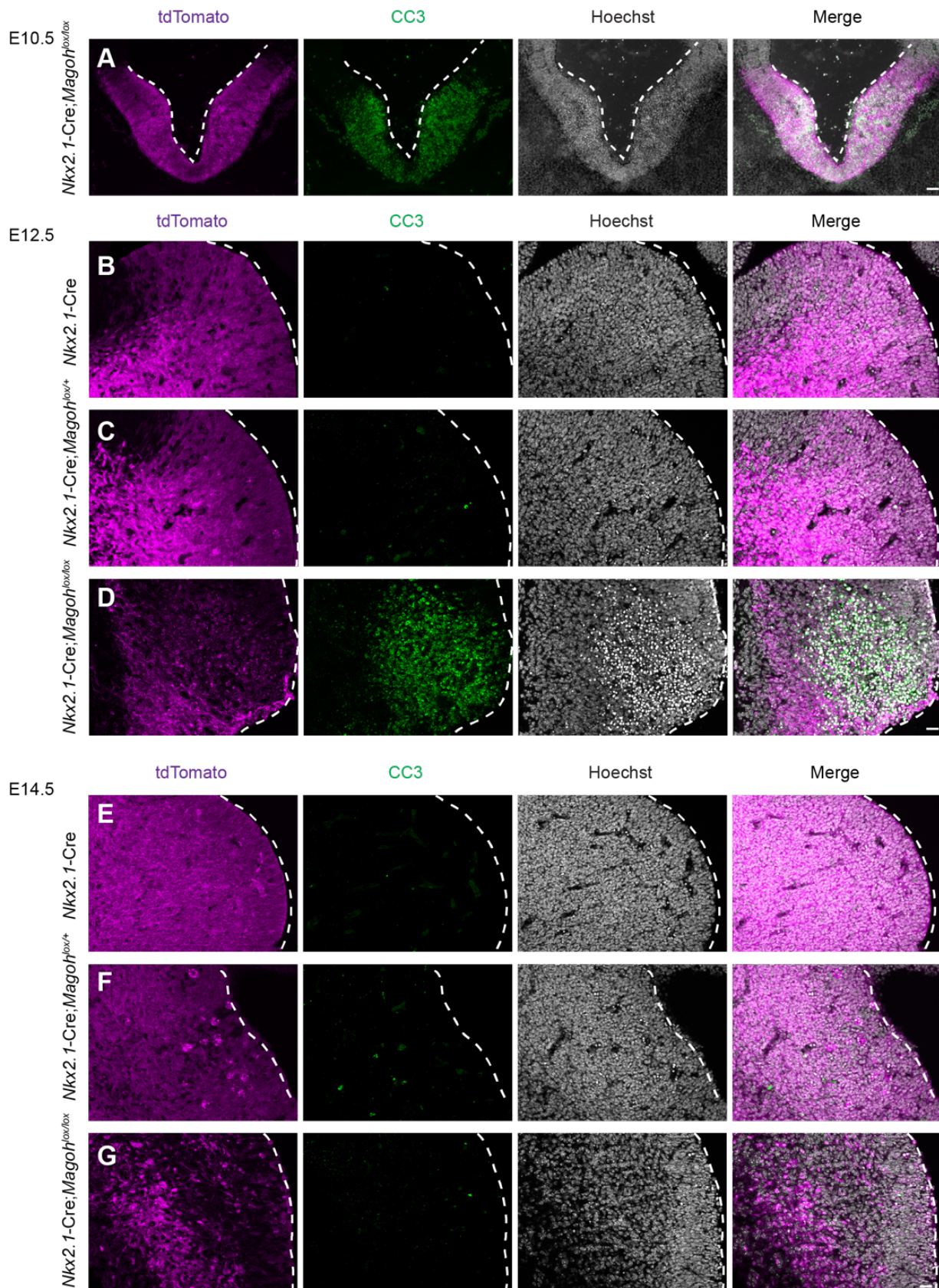


Fig. S4. *Magoh* depletion within interneuron progenitors causes apoptosis. (A-G) Coronal sections of E10.5 **(A)**, E12.5 **(B-D)**, and E14.5 **(E-G)** MGE from *Nkx2.1-cre; Magoh^{lox/lox};Rosa^{loxSTOPloxtdTomato}* **(A,D,G)** *Nkx2.1-cre;Rosa^{loxSTOPloxtdTomato}* **(B,E)**, and *Nkx2.1-cre; Magoh^{lox/+};Rosa^{loxSTOPloxtdTomato}* **(C,F)** embryos with tdTomato representing cre-recombinase expressing cells (magenta) immunostained for cleaved caspase 3 (CC3)(green), an apoptosis marker, and Hoechst (white/middle). Scale bars: **A**, 50 μ m; **B-G**, 25 μ m.

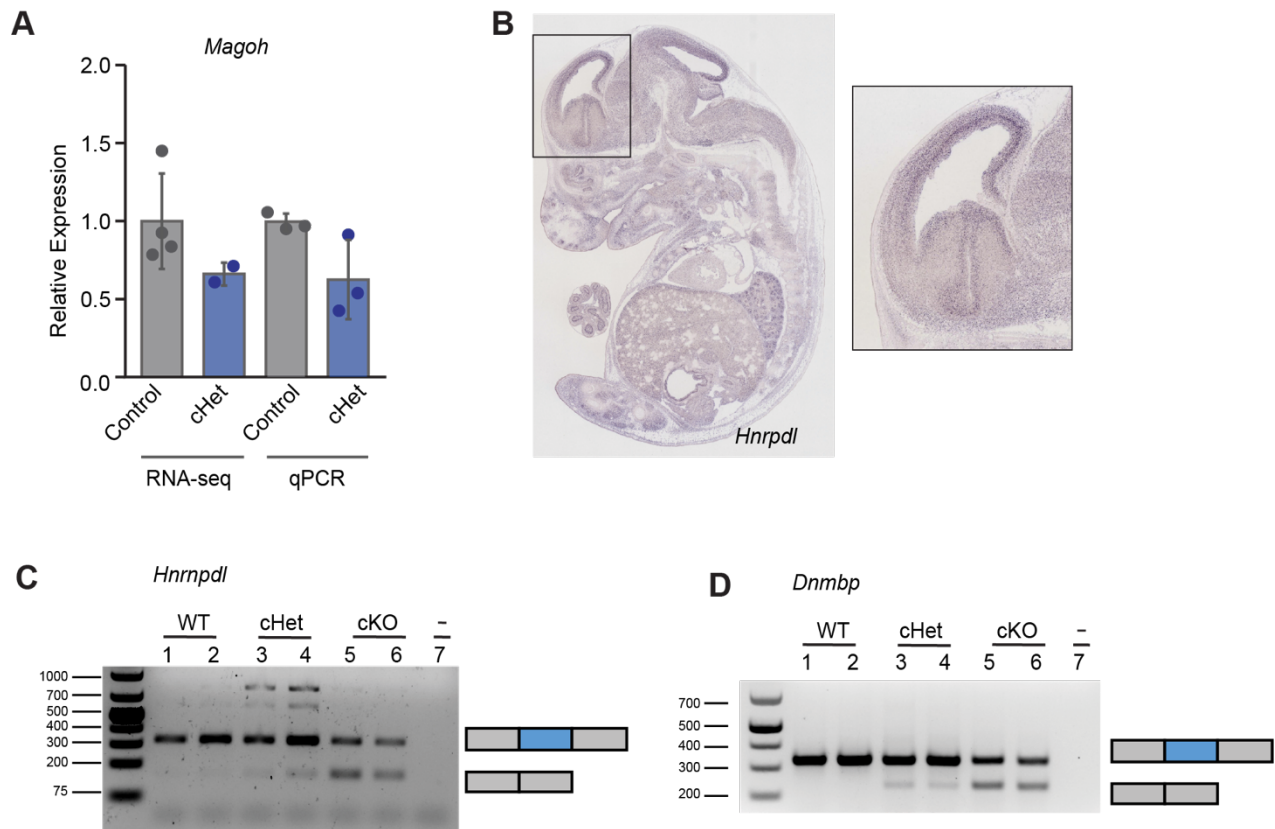


Fig. S5. Transcriptome and splicing analysis of *Magoh* depleted interneuron progenitors.

(A) *Magoh* mRNA relative expression in control and conditional heterozygotes by RNA-sequencing and RT-qPCR ($n = 4$ control and $n = 2$ heterozygotes for RNA-seq and $n = 3$ per condition for RT-qPCR). Individual dots represent biological replicates and all error bars are standard deviation (SD). **(B)** Image depicting *Hnrpd1* expression in the ganglionic eminence (Visel et al., 2004). **(C, D)** RT-PCRs depicting altered splicing of *Hnrpd1* (C) and *Dnmbp* (D) in the WT, cHet and cKO FACS-isolated interneurons. The lane numbers refer to different biological samples for the genotype listed above. The cartoon representations on the right of each gel illustrate mRNA isoforms that either include (top) or exclude (bottom) the exon. These are located adjacent to the expected bands in the gel.

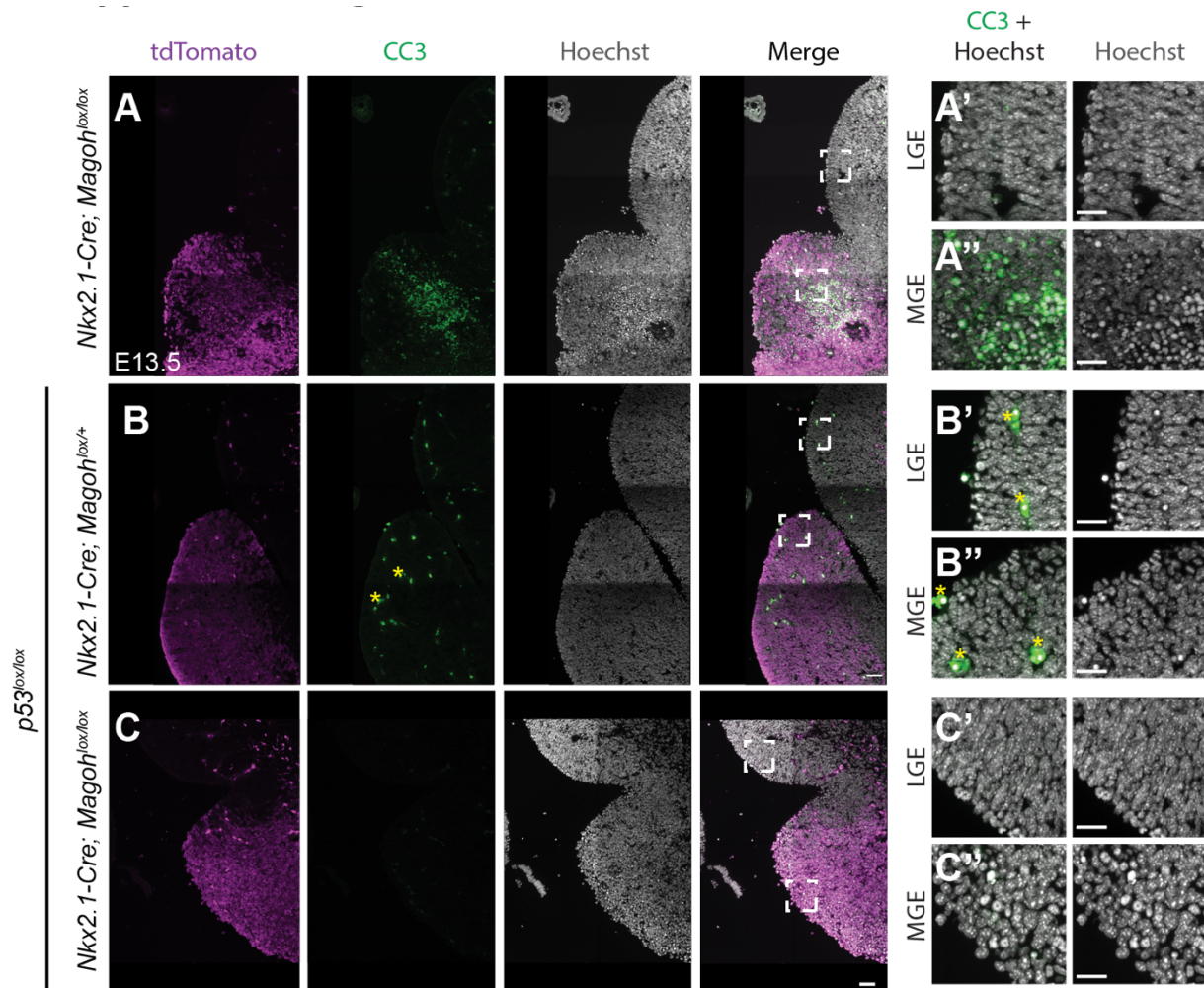


Fig. S6. *p53* conditional knockout rescues apoptosis but does not rescue mitotic delay of *Magoh* cKO. (A-C) Coronal sections of E13.5 *Nkx2.1-cre; Rosa^{loxSTOPlaxtdTomato}* (A), *Nkx2.1-cre; Rosa^{loxSTOPlaxtdTomato}; p53^{lox/lox}; Magoh^{lox/+}* (B), and *Nkx2.1-cre; Rosa^{loxSTOPlaxtdTomato}; p53^{lox/lox}; Magoh^{lox/lox}* (C) embryos immunostained for cleaved-caspase 3 (CC3, green) and Hoechst (white). (A'-C') High magnification images of regions highlighted in top and bottom of images in (A-C) depicting apoptosis evident in the MGE, but not the LGE (which was not targeted by Cre). Scale bars: A-C, 25 μ m.